International Journal of Mechanical, Industrial and Aerospace Sciences
ISSN: 2517-9950
Vol:5, No:8, 2011

A Study on the Location and Range of Obstacle Region in Robot's Point Placement Task based on the Vision Control Algorithm

Jae Kyung Son, Wan Shik Jang, Sung hyun Shim and Yoon Gyung Sung

***Abstract*—**This paper is concerned with the application of the vision control algorithm for robot's point placement task in discontinuous trajectory caused by obstacle. The presented vision control algorithm consists of four models, which are the robot kinematic model, vision system model, parameters estimation model, and robot joint angle estimation model.When the robot moves toward a target along discontinuous trajectory, several types of obstacles appear in two obstacle regions. Then, this study is to investigate how these changes will affect the presented vision control algorithm.Thus, the practicality of the vision control algorithm is demonstrated experimentally by performing the robot's point placement task in discontinuous trajectory by obstacle.

***Keywords*—**vision control algorithm, location of obstacle region, range of obstacle region, point placement

I. Introduction

THE robot using feedback visual information needs the calibration between robot and vision system at instant time when robot moves toward a target. Accordingly, calibration of cameras location, direction and focal length is most important factor [4]-[7]. But, initial calibration is not effective if position and orientation of camera change during robot manipulation. Even though the feedback of visual information overcomes difficulties to robot manipulation in some degree, it is difficult using visual feedback information if robot is interrupted by obstacle during maneuver.

Thus, this study is to present the practical vision control algorithm to solve problems mentioned above. Also, this presented algorithm is to make the robot move actively, even if relative position between camera and robot are unknown. The parameter estimation model and joint angle estimation model in the presented algorithm have form of nonlinear equation. Particularly, joint angle estimation model is includes a lot of constraints.

From our pre-studies, two important points are obtained. The first result is that the optimal number of cameras is 3 for the presented control algorithm because of a lot of constraints in joint-angle estimation model [8]. The second result is that camera placement does not affect the robot position control, but it is desirable to place cameras intensively between 2m ~ 2.5m in the robot movement direction [9].

Therefore, three cameras are intensively placed between 2m~2.5m in the robot movement direction in this study.

To carry out the study, obstacle regions are classified into two ways; first, the region A located in the middle of robot's trajectory, second, the region B located near a target. According to the change of the number of obstacles, each obstacle region involves several types of obstacles.

Thus, this study is to investigate how these changes will affect the presented vision control algorithm. The practicality of the vision control algorithm is demonstrated experimentally by performing the robot's point placement task in discontinuous trajectory by obstacle.

Jae-Kyeong Son is with Graduate school of Mechanical Engineering, Chosun University, Gwangju, South Korea. (e-mail: son0217@paran.com).

Wan-Shik Jang is with the Department of Mechanical Engineering, Chosun University, Gwangju, South Korea. (Corresponding author, phone: +82-62-230-7212; e-mail: wsjang@chosun.ac.kr)

Yoon Gyung Sung is with the Department of Mechanical Engineering, Chosun University, Gwangju, South Korea.

Sung-hyun Shim is with Undergraduate school of Mechanical Engineering, Chosun University, Gwangju, South Korea.

II. Robot vision control algorithm

In this study, the presented robot vision control algorithm is configured of four models, which are robot kinematic model, vision system model, parameter estimation model and robot joint angle estimation model. Fig. 1 shows the overall flow of vision control algorithm involved parameter and joint angle estimation model. Each model is explained in section A ~ section D.

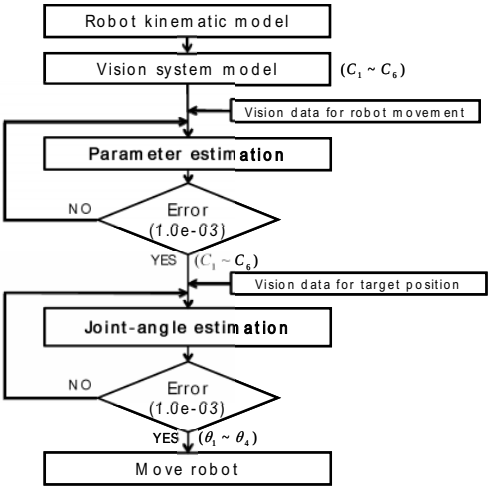

Fig. 1 Overall flow of robot's vision control algorithm

A. Robot kinematic model

Fig. 2 shows the four-axis scara type Samsung robot used in this study, and equation (1) represents the physical position of point P with respect to the base cartesian coordinate[1][11].

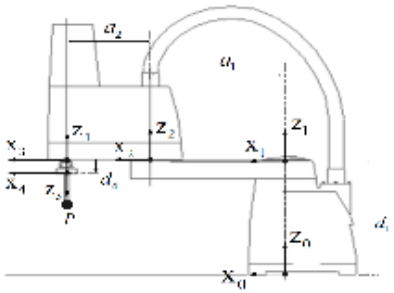

Fig. 2 Geometric configuration of Samsung SM7 4-axis robot

$$\begin{aligned} F_x &= \cos(\theta_1+\theta_2+\theta_4)P_x - \sin(\theta_1+\theta_2+\theta_4)P_y \\ &\quad + a_2(\theta_1+\theta_2) + a_1\cos\theta_1 \\ F_y &= \sin(\theta_1+\theta_2+\theta_4)P_x + \cos(\theta_1+\theta_2+\theta_4)P_y \\ &\quad + a_2(\theta_1+\theta_2) + a_1\cos\theta_1 \\ F_z &= P_z + d_1 - d_3 - d_4 \end{aligned} \quad (1)$$

Where, a_1 (=400mm), a_2 (=250mm), d_1 (=387mm), d_4 (= 67.05mm) represent Denavit-Hartenberg link factors, and $\theta_1, \theta_2, d_3, \theta_4$ are robot's joint angle. P_x, P_y, P_z are positions from the origin of last joint angle coordinate to arbitrary point P, which is given in equation (2).

$$(P_x, P_y, P_z) = (0, 0, -46.6) \quad (2)$$

B. Vision system model

The vision system model involves six parameters. These parameters represent not only uncertainty of camera position, orientation and focal length but also transformation relationship between 2-D camera coordinate and 3-D physical coordinate when the robot moves.

Vision system model defined by 2×3 matrix is given in equation (3) in order to transform 3-D physical space into 2-D camera coordinate[8]-[11].

$$\begin{bmatrix} X_m \\ \\ Y_m \end{bmatrix} = \begin{bmatrix} C_{11} & C_{12} & C_{13} \\ \\ C_{21} & C_{22} & C_{23} \end{bmatrix} \begin{bmatrix} F_x \\ F_y \\ F_z \end{bmatrix} + \begin{bmatrix} C_5 \\ \\ C_6 \end{bmatrix} \quad (3)$$

Where,

$C_{11} = C_1^2 + C_2^2 - C_3^2 - C_4^2$, $C_{12} = 2(C_2C_3 + C_1C_4)$,

$C_{13} = 2(C_2C_4 - C_1C_3)$, $C_{21} = 2(C_2C_3 - C_1C_4)$,

$C_{22} = C_1^2 - C_2^2 + C_3^2 - C_4^2$, $C_{23} = 2(C_3C_4 + C_1C_2)$

Where, X_m and Y_m represents point P of robot's end effector in 2-D camera coordinate. And among six-parameters, $C_1 \sim C_4$ account for camera direction and focal length, and $C_5 \sim C_6$ account for relative position between camera and robot.

C. Parameter estimation model

Six parameters $C_k (k = 1 \sim 6)$ included vision system model are obtained by means of minimization of following performance index.

$$J(C_k) = \sum_{i=1}^{n} \left[X_m^i - X_c^i \right]^2 + \left[Y_m^i - Y_c^i \right]^2 \quad (4)$$

Where, n is the number of measurement data, and X_c, Y_c represents the measured value in x, y camera coordinate.

Minimizing equation (4) by Newton-Raphson method, the parameter estimation model is given as follows [2][11].

$$C_{k,j+1} = C_{k,j} + \Delta C \quad (5)$$

Where, $\Delta C = (A^T W A)^{-1} A^T W R$, A is jacobian matrix, R is residual vector, j is number of iteration and W is weight matrix used an unit matrix in this paper.

Parameters are obtained by iteration method as equation (5).

D. Robot joint angle estimation model

Based on the estimated six-parameters from parameter estimation model about each camera, joint angles $\theta_i (i = 1 \sim 4)$ with respect to target position are obtained by means of minimization of following performance index.

$$\begin{aligned} J(\theta_i) = \sum_{q=1}^{3} &\left[X_m^q(F_x(\theta_i), F_y(\theta_i), F_z(\theta_i); C_k^q) - X_t^q \right]^2 \\ &+ \left[Y_m^q(F_x(\theta_i), F_y(\theta_i), F_z(\theta_i); C_k^q) - Y_t^q \right]^2 \end{aligned} \quad (6)$$

Where, $q(1-3)$ is the number of camera, $k(1-6)$ represents the number of parameter. Also, X_t^q and Y_t^q represent the target camera coordinate in q-th camera, X_m^q and Y_m^q represent the values of vision system model using the estimated parameter values about each camera.

As explained in section C, the joint angle estimation model by Newton-Raphson method to minimize equation (6) is given as follows.

$$\theta_{i,j+1} = \theta_{i,j} + \Delta\theta \quad (7)$$

Where, $\Delta\theta = (B^T W B)^{-1} B^T W R$, B is jacobian matrix, R is residual vector, j is number of iteration and weighting matrix W is an unit matrix.

Joint angles are obtained by iteration method as equation (7), and use to move toward a target.

III. Experimental Apparatus and Method

A. Experimental apparatus

The experimental apparatus consists of vision system, robot system and host PC as shown in Table I and Fig. 3.

TABLE I
SPECIFICATION OF EXPERIMENTAL APPARATUS

System	Specification	
Vision System	CCD Camera	Sony XC-ES51
		Avenir TV zoom lens
	Vision Board	MATROX monochrome meteor2-MC4
		Resolution : 640 × 480
		Gradation 256
		Maximum Sampling rate 30MHz
	Library	Matrox Imaging Library 8.0DEV
Robot System	Robot	Samsung SM7 4-axis Robot
	Robot controller	MMC-BDPO41PNB
PC	• Industrial MB800V	
	• CPU : 2.8GHz	
	• 512MB	

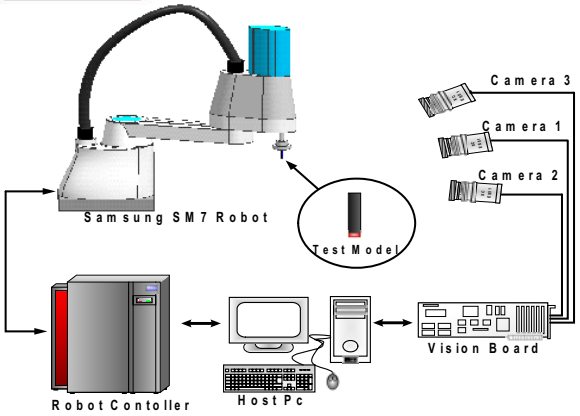

Fig. 3 Experimental set-up

B. Experimental Procedures

Robot's point placement experiment performed in two regions; first, region A located in the middle of robot's trajectory, second, region B located near a target. According to the change of the number of obstacles, each obstacle region involves several types of obstacles. Then, this study is to investigate how these changes will affect the presented vision control algorithm.According to the pre-studies [8][9], three cameras are intensively placed between 2.0m~2.5m in the robot's movement direction. And experimental procedures are as follows.

1) Set up 21 movement steps of arbitrary robot's trajectory.
2) Set up two obstacle regions in robot's trajectory.
3) Set up several types of obstacles in each obstacle region, as shown in Table II.
4) Estimate the parameters and the robot joint angles to the several types of obstacles in obstacle region A and B when the robot moves toward a target along discontinuous trajectory.
   - Estimate the parameters ($C_1 \sim C_6$) about each camera, based on the acquired vision data during robot movement.
   - Estimate the robot joint angles with respect to target position from joint angle estimation model, based on the estimated six-parameters in each camera.
5) Investigate the precision of robot's point placement task after the robot reaches a target using the estimated joint angles.

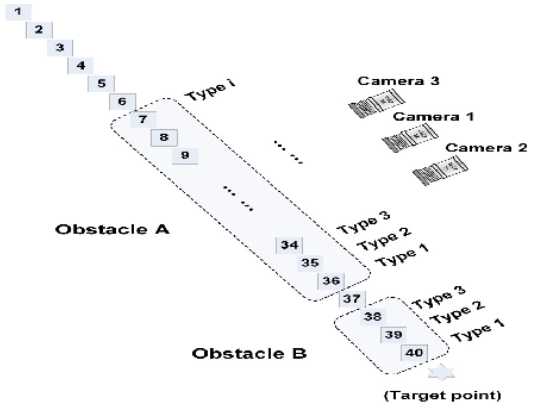

Fig. 4 Obstacle regions in robot's trajectory

TABLE II
THE TYPES IN EACH OBSTACLE REGION

Type #	Type 1	Type 2	Type 3	•••	Type i
# of obstacle	1	2	3	•••	i

IV. Experimental Result for Vision System Model's Suitability

The error between the actual vision data and the estimated results of the vision system model in each camera is defined as r.m.s. in equation (8) [3].

$$e_{rms} = \sqrt{\frac{\sum_{i=1}^{n}\left\{\left(e_x^i\right)^2 + \left(e_y^i\right)^2\right\}}{n}} \tag{8}$$

Where, e_x and e_y are errors between the actual vision data and the estimated results of vision system model in x and y coordinate, n is the number of steps that vision data acquired when the robot moves toward a target.In Fig. 5~Fig. 7, the symbols (□ ,○ ,◇) represent an actual vision data measured from each camera while the robot moves toward a target, and the symbols (+, ×, *) represent the estimated results of the vision system model in each camera, based on the parameter estimation model.

A. The case with no obstacle region

While the robot moves toward a target along the continuous trajectory with 21steps without obstacle region, the actual vision data of 21steps acquired during movement are similar to the estimated results of vision system model based on the parameter estimation model as shown in Fig. 5.Using equation (8), error values in each camera are found to be approximately ±0.001pixel ~ ±1.134pixel.

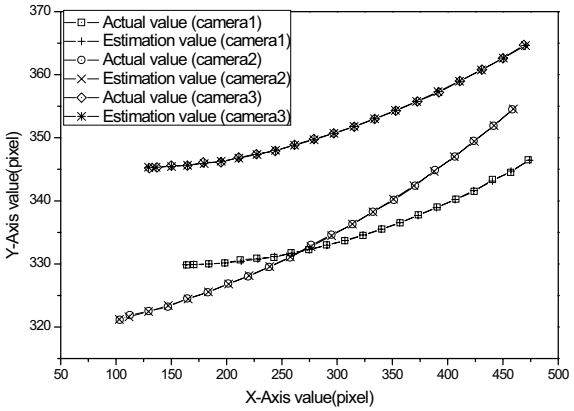

Fig. 5 Comparison of the actual and estimated values in no obstacle region

B. The case with the obstacle region

The obstacle regions are classified into two categories. First, region A located in the middle of robot's trajectory, region B located near a target. Table 2 shows several types of obstacles in each region.

Fig. 6-7 show the experimental results in each obstacle region, and the shade parts of each figure show the case which the camera did not acquired the vision data.

1) Obstacle region A: middle

Fig. 6 shows the comparison of the estimated results of vision system model and the actual vision data in each camera when the obstacle exists in 50% range (type 11) of robot's trajectory. Then, the compared results of type 11 are very similar. Even though only the results of type 11 show in this paper, similar results are obtained for all types.

Using equation (8), error values of all types are obtained as approximately ±0.003pixel~±0.797pixel. The reason is that enough compensation is achieved by the acquired vision data of next steps, even though the vision data can not be acquired by obstacle in 50% range of robot's trajectory.

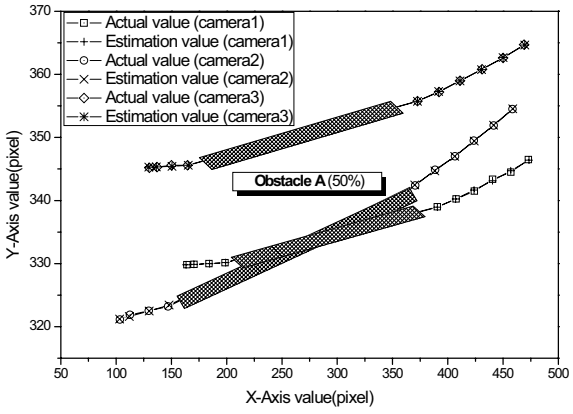

Fig. 6 Comparison of the actual and estimated values for type11 in the obstacle region A

2) Obstacle region B: near a target

Fig. 7 shows that the compared results between actual vision data and estimated results of vision system model in the obstacle region B near a target.

The errors between the actual vision data and the estimated results of vision system model in each camera are calculated using the r.m.s. defined in equation (8). Errors in all types are in the range of ±0.006pixel~±0.931pixel, even though only the results of type11 show in this paper.

The estimated results of vision system model in obstacle region B have nearly the similar to those of the no obstacle region, because the data is acquired in all steps before reaching an obstacle near a target.

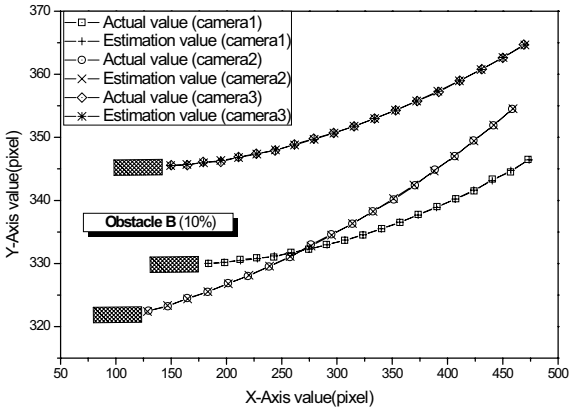

Fig. 7 Comparison of the actual and estimated values for type3 in the obstacle region B

V. Experimental Results for Robot's Point Placement Task

When the robot moves toward a target along discontinuous trajectory, the number of obstacle changes in two obstacle regions. Then, this study is to investigate how these changes will affect the presented vision control algorithm.

For this experiment, the robot joint angles are calculated by the joint angle estimation model using six estimated parameters. Then, the precision of robot's point placement task is investigated after the robot reaches a target using the estimated joint angles.

Robot's point placement experiments are performed in two obstacle regions; first, region A located in the middle of robot's trajectory, second, region B located near a target.

After the robot reaches a target, the error between the robot's position measured from encoder values and actual target position is defined as r.m.s in equation (9) [3].

$$e_{rms} = \sqrt{\frac{(e_x)^2 + (e_y)^2 + (e_z)^2}{3}} \qquad (9)$$

Where, e_x, e_y and e_z are errors in x, y and z coordinate, respectively.

A. The case with no obstacle region

When the robot reaches a target to execute point placement task experiment without obstacle region, table III shows the

comparison of the measured robot position values and actual target position values. Then, the error of robot's point placement task is ±0.505mm.

TABLE III
FOR NO OBSTACLE, COMPARISON OF THE ACTUAL AND MEASURED VALUE FOR TARGET POSITION IN X-Y-Z COORDINATE

Obstacle region	Fx(mm)	Fy(mm)	Fz(mm)	error
No obstacle	513.356	-242.912	132.337	0.505
Real value	512.949	-243.686	132.300	

B. The case with the obstacle region

1) Obstacle region A: middle

As shown in Fig. 8, the errors of each obstacle type in region A located in the middle of robot's trajectory are ±0.504mm~± 0.577mm. And these results have similar to those of no obstacle region. Namely, these results show that robot's point placement task is successfully achieved when the obstacles exist within 50% range of robot's trajectory. The reason is that enough compensation is achieved by the acquired vision data of next steps, even though the vision data can not be acquired by obstacle at that time.

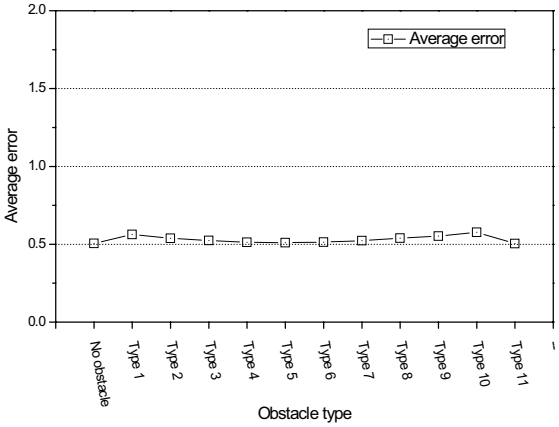

Fig. 8 For Obstacle region A, comparison of the average errors

2) Obstacle region B: near a target

As shown in Fig. 9, the errors of three types in the obstacle region B located near a target are ±0.639mm in type1, ±0.923mm in type2 and ±1.218mm in type3. These results show that the error increases as the range of obstacle near a target increases. The reason is that any data can not be acquired for compensation, unlike region A.

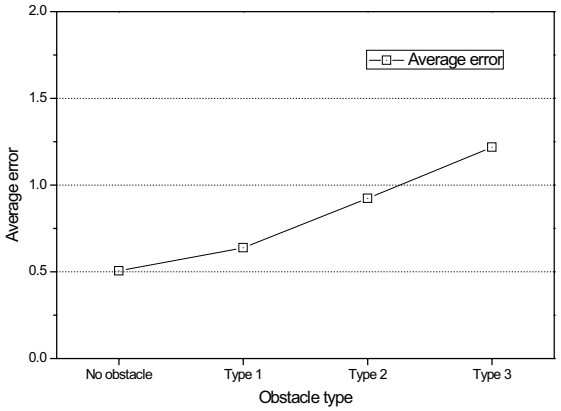

Fig. 9 For obstacle region B, comparison of the average errors

VI. CONCLUSION

This paper is focused on how location and range of obstacle region will affect the presented vision control algorithm by performing the experiments for robot's point placement task. The obtained results are summarized as follows.

1) Experimental study in region A shows that the robot's point placement task is achieved successfully with error of ± 0.504mm~±0.577mm when the obstacles exist within 50% range of robot's trajectory. These results are very close to those of no obstacle region.

2) Experimental study in region B shows that the robot's point placement is achieved successfully with error of ±1.0mm within 10% of robot's trajectory. Unlike region A, these results show that the errors increase as the range of obstacle region increases.

3) As a result, region A has better result than obstacle region B near a target because enough compensation is achieved by the acquired vision data of next steps, even though vision data can not be acquired by obstacle at that time.

REFERENCES

[1] J. C. John, *Introduction to Robotics mechanics and control*, 2nd ed., U.S.A: Addison-Wesley, 1989, pp. 84.
[2] J. L. Junkins, *An Introduction to Optimal Estimation of Dynamical Systems*, Sijthoff and Noordhoff, Alphen Aan Den Rijn, 1978, pp. 29~33.
[3] F. David, P. Robert, and P. Roger, *Statistic*, Canada: W.W.Norton, 1978, pp.58~59.
[4] R. Kelly, R. Carelli, O. Nasisis, B. Kuchen, and F. Reyes, "Stable Visual servoing of camera-inhand robotics systems," *IEEE/ASME Trsns. on Mechatronics*, Vol. 5, No. 1, pp. 39~48, 2000.
[5] T. Yoshihiro, K. Yasuo, and I. Hiroyuki, "Positioning-Control of Robot Manipulator Using Visual Sensor," *Int. Conference on Control, Automation, Robotics and Vision*, pp.894 ~ 898, 1996.
[6] H. Bacakoglu, M. Kamel, "An Optimized Two-Step Camera Calibration Method," *Proceedings of the 1997 IEEE International Conference on Robotics And Automation*, pp.1347~ 1352, 1997.
[7] S. Machiko, J. K. Aggarwal, "Estimation of Position and Orientation from Image sequence of a Circle," *IEEE International Conference on Robotics and Automation*, pp.2252~ 2257, 1997.
[8] W. S. Jang, K. S. Kim, K. Y. Kim, and H. C. Ahn, "An Experimental Study on the Optimal number of Cameras used for Vision Control System," *KSMTE*, Vol. 13, No. 2, pp. 94~103, 2004.

[9] K. U. Min, W. S. Jang, "An Experimental Study on the Optimal Arrangement of Cameras used for the Robot's Vision Control Scheme," *KSMTE*, Vol. 19, No. 1, pp. 15~25, 2010.
[10] J. K. Son, W. S. Jang, and K. U. Min, "An experimental study on the effectiveness of robot vision control scheme in discontinuous robot's trajectory caused by obstacle" *KSPE Spring Conference*, pp. 127~128, 2009.
[11] J. K. Son, *An experimental study on the practicality of vision control scheme used for robot's point placement task in discontinuous trajectory*, A thesis for master's degree, Chosun University, Republic of Korea, 2010.